IFSCC 2025 full paper (IFSCC2025-592)

Research on the Development and Stability of the Critical Emulsion System

Jiacheng Wang[1], Hongxia Wang[1], Jihua Wei* [2], Hongxiu Liao[1], Wenxu Qi[1], Yuyan Chen[1], Jingxia Sun[1], Bokai Jiang[1], Peiwen Sun[1]

[1] Research & Innovation Center, [2] International Academy of science, Proya Cosmetics Co. Ltd, Hangzhou, China

1. Introduction.

With the transformation of the Chinese skincare market from a "functionality-first" to a "safety-first" approach, the unique needs of sensitive skin populations are reshaping the industry landscape. According to the "China Women's Sensitive Skin In-depth Analysis and Sensitive Makeup Research Report," the proportion of women with sensitive skin in China is now approaching 60%. This figure highlights the significant contradiction between the high emulsifier content in stable emulsification systems and the fragile skin population. This poses a fundamental challenge to the development of water-in-oil emulsification systems. The addition of extra emulsifiers can increase the risk of skin irritation [1-2]. Meanwhile, the Chinese skincare market has an extreme pursuit of excellent skin feel. The sticky residue caused by excessive addition of emulsifiers is in fundamental conflict with the "zero presence" experience advocated by the new generation of consumers. Additionally, as consumer demand for moisturizing effects becomes more prominent, increasing the introduction of solid oils to enhance product moisturizing performance has become an important direction for industry development [3-4]. Against this backdrop, the development of high-wax-content critical emulsification systems has become a key to the development of the Chinese skincare market.

It is worth noting that the leapfrog development of China's e-commerce infrastructure is bringing new challenges to critical emulsification systems. According to the “2024 China Skincare Consumption Trend Report”, the proportion of cosmetics sold online has exceeded 50%, and the logistics network coverage rate has reached 98%. However, In extreme transportation environments, high temperatures can lead to more intense molecular thermal motion, reduced intermolecular forces, and decreased interfacial tension, resulting in reduced stability [5]. In extremely cold environments, the crystallization of the aqueous phase can increase the possibility of interfacial membrane damage, this situation poses a challenge to the stability of products with critical emulsification systems [6].

This study, in combination with the demands of the Chinese cosmetics consumer market and the current state of logistics transportation, explores a method to stabilize high-wax-content

critical emulsification systems through process control. It also demonstrates that the rational configuration of process parameters can play a positive role in the effectiveness of products, providing new technological support for the skincare production industry.

2. Materials and Methods

2.1 Preparation of High-Wax Content Critical O/W Emulsion

The sample formulation is shown in Table 1. Phase A represents the aqueous phase, which includes emulsifying stabilizers, chelating agents, humectants, and other components. Phase B represents the oil phase, mainly consisting of emulsifiers, waxes, and a small amount of liquid oils.

Table 1. Formula information of high wax content critical O/W emulsion

Phase	Ingredient（INCI）	Formula content (%)
A	WATER	To 100
	AMMONIUM ACRYLOYLDIMETHYLTAURATE/VP COPOLYMER	0.11%
	SODIUM POLYACRYLATE STARCH	0.11%
	DISODIUM EDTA	0.04%
	1,2-HEXANEDIOL	0.43%
	PROPANEDIOL	4.57%
	GLYCERYL GLUCOSIDE	0.45%
	GLYCERIN	0.45%
	DIPROPYLENE GLYCOL	1.14%
B	GLYCERYL STEARATE CITRATE	0.46%
	POLYGLYCERYL-3 METHYLGLUCOSE DISTEARATE	0.11%
	SORBITAN STEARATE	0.17%
	CETEARYL ALCOHOL	2.97%
	LIMNANTHES ALBA (MEADOWFOAM) SEED OIL	0.06%
	CAPRYLIC/CAPRIC TRIGLYCERIDE	0.57%

After completely dissolving and dispersing the ingredients of Phase A, heat them to 80°C. Place the ingredients of Phase B in a water bath and heat to 80°C. Mix Phases A and B together, then adjust the total weight to 100% with water. Place the mixture on an IKA stirrer (IKA, K25-S25N, Germany) and stir at 600 rpm for 5 minutes to ensure uniform mixing. Maintain the temperature at 80°C and use an IKA homogenizer to emulsify the mixture at different speeds: 4000 rpm, 6000 rpm, 8000 rpm, 10000 rpm, 12000 rpm, and 14000 rpm, with each emulsification lasting for 5.5 minutes. After emulsification, stir and cool the mixture to 35°C, then stop stirring and store the samples in a constant-temperature chamber at 25°C.

2.2 Microscopic Structure Observation of Emulsions

The microscopic morphology of high-wax-content critical emulsions prepared at different homogenization speeds was observed using a polarized light microscope (LABOMED, Lx POL, USA). The ordinary optical and polarized light structures of the samples were observed using

a 10x eyepiece and a 100x objective lens after the samples had been placed in a 25°C constant-temperature chamber for 24 hours.

2.3 Particle Size Analysis

The particle size distribution of the samples prepared at different homogenization speeds was measured using a laser particle size analyzer (Anton Paar, Litesizer DLS 500, Austria). Prior to testing, the prepared samples were stored in a constant-temperature chamber at 25°C for 24 hours. For the test, the samples were diluted with deionized water at 25°C in a 1:100 ratio, then transferred to a cuvette and placed into the measurement cell. The particle size of the samples was measured, with three replicate tests conducted.

2.4 Zeta Potential Analysis

The stability of the samples at different temperatures was characterized using zeta potential measurements, conducted with a laser particle size analyzer (Anton Pear, Litesizer DLS 500, Austria). Before testing, the prepared samples were stored in constant-temperature chambers at 5°C, 25°C, and 45°C for 24 hours. For the test, the samples were diluted with deionized water at 5°C, 25°C, and 45°C in a 1:200 ratio, then transferred to an omega sample cell and placed into the measurement cell. The equilibrium temperature was set according to the test temperature, and the zeta potential of the samples was measured, with three replicate tests conducted.

2.5 Viscosity Testing

Viscosity testing was conducted using a viscometer (Brookfield, DV2T, USA) equipped with a spindle. The prepared samples were stored in a constant-temperature chamber at 25°C for 24 hours before testing. A No. 91 spindle was used at a rotational speed of 6 rpm, with a testing duration of 15 seconds to measure the viscosity of the samples after 24 hours of preparation.

2.6 Rheological Behavior Testing

The rheological behavior of the samples was analyzed using a rheometer (HR20 Discovery, TA, USA). A 1° parallel plate was used for the tests. The prepared samples were stored in a constant-temperature chamber at 25°C for 24 hours and allowed to equilibrate for 5 minutes before each test.

Small-Amplitude Oscillatory Shear (SAOS) Scan: The linear viscoelastic region of the prepared samples was determined by dynamic strain scanning at a fixed frequency of 1 Hz, with a stress scan ranging from 0.01% to 100%.

Temperature Sweep: The temperature program was set to hold at 6°C for 2 minutes, followed by heating to 65°C at a rate of 5°C/min, with a strain of 0.1% and a frequency of 1 Hz.

2.7 Thermodynamic Behavior (DSC) Testing

The thermodynamic behavior of the samples was analyzed using Differential Scanning Calorimetry (DSC). Approximately 5–8 mg of the emulsion sample was placed in a dedicated crucible. The scanning program was set to hold at -5°C for 5 minutes, then heat to 80°C at a rate

of 5°C/min to obtain the melting curve. The sample was held at 80°C for 2 minutes, followed by cooling to -5°C at a rate of 5°C/min to obtain the crystallization curve.

2.8 Sensory and Efficacy Testing

To further investigate the impact of process parameters on the efficacy and sensory feel of the emulsions, a professional sensory evaluation panel first tested the product's texture and usage feel. Subsequently, a hydration performance test was conducted on 24 healthy volunteers. The changes in the moisture content of the stratum corneum of human skin after using the cosmetic products were measured and analyzed using a capacitive skin moisture analyzer. The samples were applied at a dosage of (2.0 ± 0.1) mg/cm² in a single application. Latex finger cots were used to evenly spread the test samples over the designated test areas. The testing time points were before application, and at 30 minutes, 1 hour, 2 hours, 4 hours, and 8 hours after application.

3. Results

3.1 Microscopic Structure Observation of Emulsions

The microscopic structures of the prepared samples were observed under both ordinary optical and polarized light microscopy, as shown in Figure 1. For the samples homogenized at 4000 rpm, the particle size was relatively large and irregular, with many wrinkles on the surface. Under polarized light, only "Crystalline Aggregates" could be observed, rather than liquid crystalline structures. As the homogenization speed increased, the emulsion particle size gradually became more uniform, and the liquid crystalline structures became more evident. However, when the homogenization speed exceeded 12000 rpm, most of the emulsion particle sizes were below 1 μm, and aggregation of particles began to occur. Additionally, the liquid crystalline structures started to disappear under polarized light. When the homogenization speed reached 14000 rpm, the liquid crystalline structures completely vanished.

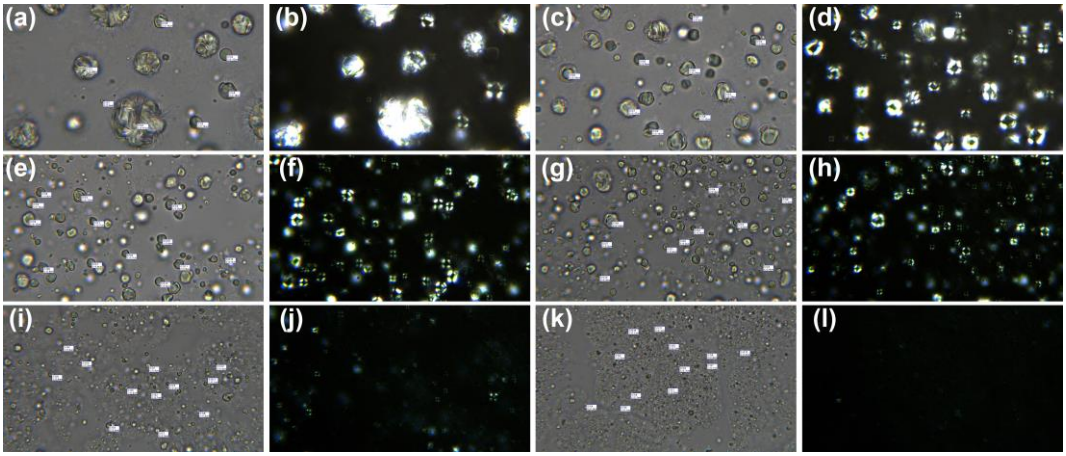

Figure1. The microstructure of samples prepared under ordinary optics (left) and the corresponding microstructure under polarized light (right) at different homogenization rates. (a) (b) 4000rpm; (c) (d) 6000rpm; (e) (f) 8000rpm; (g) (h) 10000rpm; (i) (j) 12000rpm; (k) (l) 14000rpm

3.2 Results of Particle Size, Viscosity, and Zeta Potential Tests

Stability is crucial in O/W emulsion systems. To verify the impact of process parameters on the critical system, the prepared samples were tested for particle size, viscosity, and zeta potential. Figures 2 (a)-(f) show the particle size test results. It can be observed that the particle size results for samples homogenized below 10000 rpm are consistent with the microscopic observations. However, when the homogenization speed reaches 12000 rpm and above, a new particle size distribution peak appears at 7-8 μm.

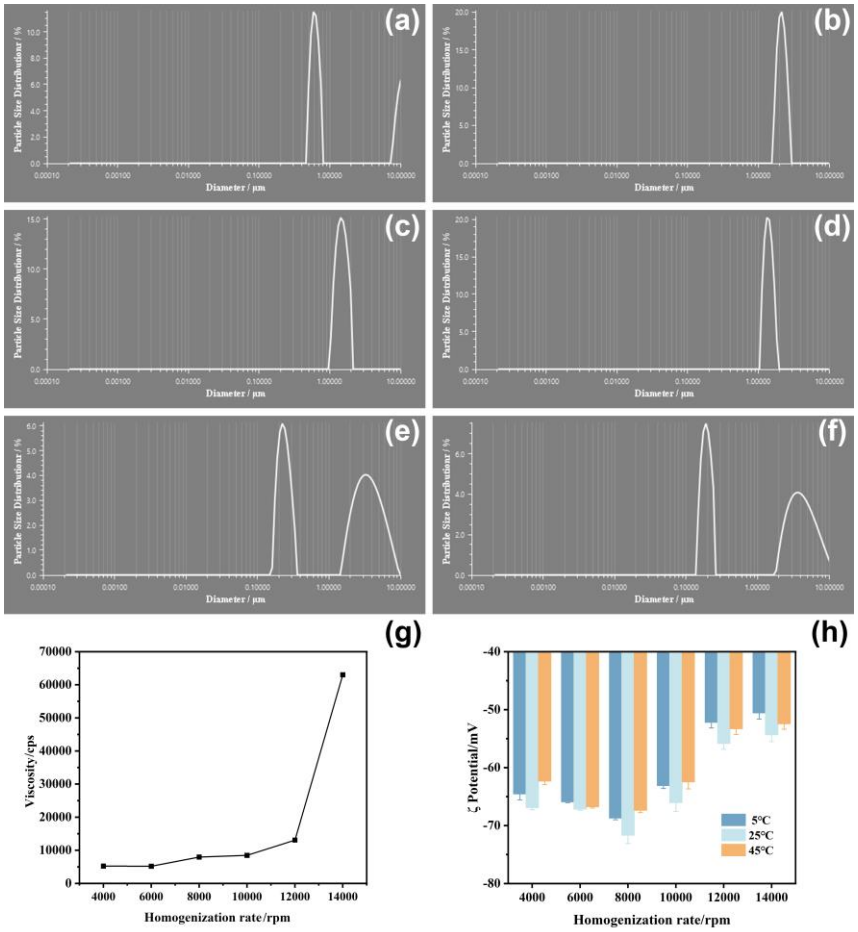

Figure 2. Particle size, viscosity and Zeta test results. (a-f)The particle size test results of the samples under different homogenization speeds; (a) 4000rpm; (b) 6000rpm; (c) 8000rpm; (d) 10000rpm; (e) 12000rpm; (f) 14000rpm; (g) The viscosity of samples prepared at different homogenization speeds; (h) The Zeta potential of samples prepared at different homogenization rates and different temperature.

Figure 2 (g) presents the viscosity test results. It is evident that before 12000 rpm, the viscosity of the samples increases in a linear relationship with the process parameters. However, when the homogenization speed reaches 14000 rpm, the viscosity increases sharply. Figure 2 (h) shows the zeta potential test results. As the homogenization speed increases, the absolute value of the zeta potential of the emulsion system at 25°C first increases and then decreases. The highest absolute value of the zeta potential is observed at 8000 rpm, indicating that the electrostatic repulsion between emulsion particles is the greatest at this speed, which is conducive to maintaining the stability of the emulsion. Additionally, the absolute values of the zeta potential of the emulsions at low and high temperatures also exhibit the same trend.

3.3 DSC Test Results

Figure 3 shows the non-isothermal crystallization and melting curves of the emulsions prepared at homogenization speeds of 8000 rpm and 14000 rpm. During the cooling process, the emulsion prepared at 14000 rpm exhibits a broad exothermic peak at 78.1°C, while the emulsion prepared at 8000 rpm does not show any such peak. Similarly, during the heating process, the emulsion prepared at 14000 rpm shows a small endothermic peak at 52.4°C, which is absent in the emulsion prepared at 8000 rpm.

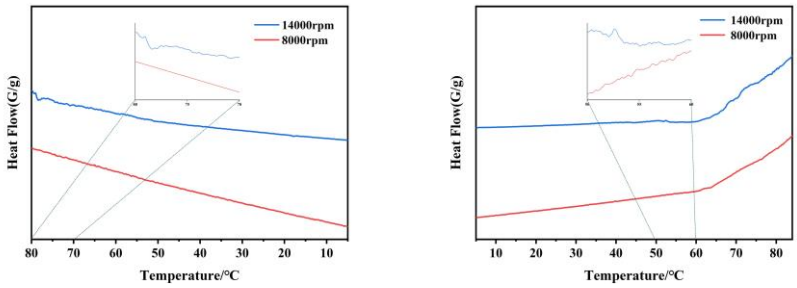

Figure 3. DSC test results of emulsions prepared by homogenization at 8000rpm and 14,000 rpm. (a) Non-isothermal crystallization curve; (b) Melting curve

3.4 Rheological Behavior Test Results

After clarifying the impact of process parameters on the emulsification stability of the critical emulsification system, further investigations were conducted to explore the effects of process parameters on the rheological behavior of the emulsions. Figure 4 (a) shows the small-amplitude oscillatory shear (SAOS) test results of the samples. The oscillatory strain curves at the "solid-to-liquid" transition under different process parameters were plotted based on the intersection points of the storage modulus (G') and loss modulus (G''). As shown in Figure 4 (b), the tolerance of the emulsions prepared at different homogenization speeds to oscillatory strain first increased and then decreased with the increase in homogenization speed. The emulsion prepared at 8000 rpm exhibited the highest tolerance to oscillatory strain.

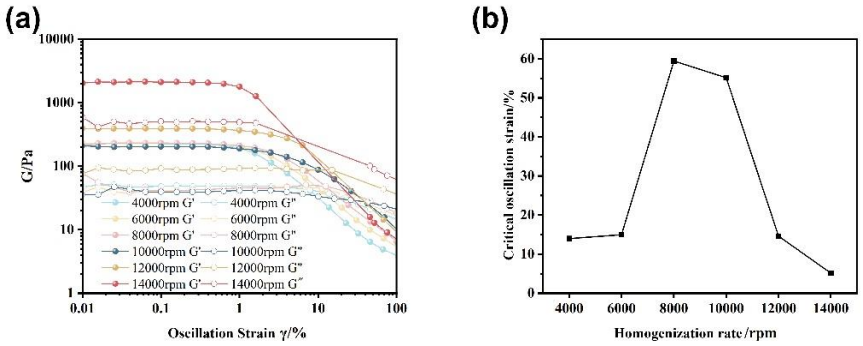

Figure 4. The oscillatory rheological behavior of samples at different homogenization speeds. (a) Stress scanning curves of samples at different homogenization speeds; (b) The yield stress of the samples at different homogenization rates

Furthermore, to verify the influence of temperature on the rheological behavior of the prepared emulsions, Figure 5 presents the temperature-dependent rheological test results. Figure 5 (a)

shows the storage modulus (G') test results. It can be observed that all samples exhibited a sudden change in G' with increasing temperature. However, it is evident that the shear tolerance of the emulsions to temperature rise significantly decreased with increasing homogenization speed. Similarly, Figure 5 (b) shows the loss modulus (G'') test results, which exhibit the same trend as G'.

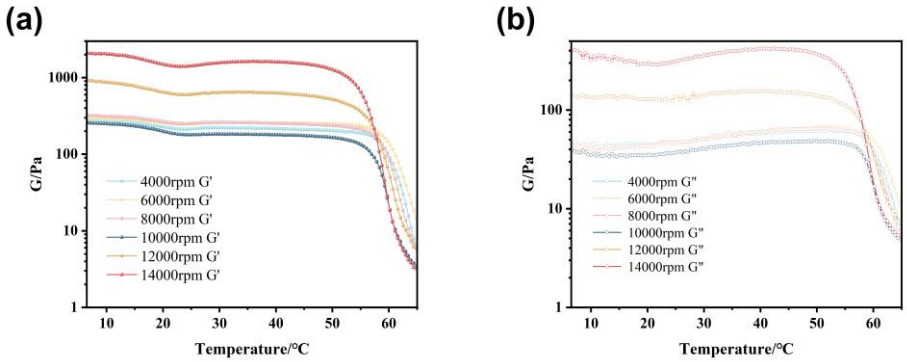

Figure 5. The variable-temperature rheological behavior of samples prepared at different homogenization rates. (a) Storage modulus(G')；(b) Loss modulus(G")

3.5 Sensory and Efficacy Test Results

Figure 6 shows the sensory and moisturizing performance test results of the samples prepared at different homogenization speeds. The sensory test results in Figure 6 (a) indicate that the sensory evaluations of samples prepared at medium and low homogenization speeds were higher than those prepared at high homogenization speeds. Among them, the samples prepared at 8000 rpm showed significant advantages in fineness, spreadability, and smoothness. The moisturizing performance test results in Figure 6 (b) clearly show that samples prepared at medium and low homogenization speeds exhibited better moisturizing properties. Specifically, the samples prepared at 8000 rpm demonstrated distinct advantages in water content and retention.

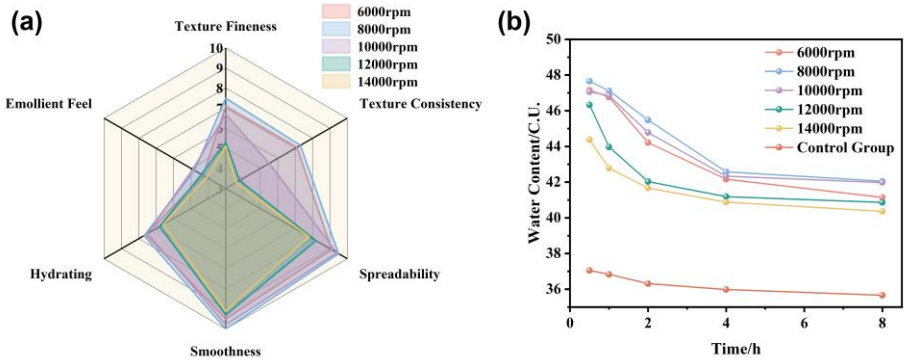

Figure 6. Sensory and efficacy test results of samples prepared at different homogenization speeds. (a) Sensory test results; (b) Moisturizing performance test results

4. Discussion

4.1 Mechanism of Process Parameters on System Stability

This study elucidated the mechanisms by which process parameters influence critical emulsification systems through multi-scale characterization. Samples prepared at low

homogenization speeds exhibited larger emulsion particle sizes, with the surface of the dispersed phase presenting a “wrinkled” appearance to increase the surface area (Figure 1). This ensured adequate coverage by the emulsifier, indicating that the available coverage area of the emulsifier exceeded the surface area of the internal phase. The zeta potential test results also show that the absolute value of zeta potential (|ζ|) for emulsions prepared at low homogenization speeds is relatively low. As the homogenization speed increases, within the range of 8000–10000 rpm, emulsions with uniform particle sizes and distinct liquid crystalline structures are obtained, accompanied by an increase in |ζ|. This confirms that when the emulsifier content can adequately cover the surface area of the internal phase, smaller emulsion particle sizes result in higher |ζ|, and the emulsions generally exhibit better stability [7-8].

When the homogenization speed was too high, the dispersed phase particles of the emulsion were excessively sheared and reduced in size, thereby increasing the surface area of the internal phase. The emulsifier content was no longer sufficient to cover the internal phase, leading to partial aggregation between particles [9]. The liquid crystalline structures began to disappear (Figure 1), The emulsion particle size distribution shifted from a single peak to a bimodal distribution, with the emergence of large particle aggregates at 7-8 μm (Figure 2). The |ζ| decreased significantly, likely due to the limited emulsifier coverage thinning the electrical double layer of the particles, thereby reducing the stability of the emulsion [10]. Additionally, the zeta potential test results at 5°C and 45°C showed that emulsions prepared under appropriate process parameters exhibited good stability at both low and high temperatures, thus better adapting to the extreme climates that may be encountered during logistics transportation in China.

Viscosity test results indicated that when the homogenization intensity was ≤12000 rpm, the viscosity of the samples increased linearly with the process parameters. This can be attributed to the reduction in particle size, which increases the number of emulsion particles per unit volume and enhances the interactions between the dispersed phase particles, leading to an increase in viscosity [11]. However, when the homogenization speed reached 14000 rpm, the viscosity increased sharply, which is related to the partial aggregation of the internal phase.

Analyzing the thermodynamic behavior of the emulsions (Figure 3), it was found that the emulsion prepared at 8000 rpm did not show any significant exothermic or endothermic peaks during heating and cooling. In contrast, the emulsion prepared at 14000 rpm exhibited an exothermic peak during cooling and an endothermic peak during heating. This can also be attributed to the insufficient emulsifier coverage of the internal phase, preventing the solid oils from forming a lamellar liquid crystalline structure at the interface [12]. As a result, solidification and melting occurred successively with the decrease and increase in temperature.

4.2 Correlation between Rheological Behavior and Process Parameters

The small-amplitude oscillatory shear (SAOS) test results (Figure 4) showed that under low oscillatory shear, all samples exhibited solid-like behavior (storage modulus G' > loss modulus G''). As the oscillatory shear strain increased, the intersection points of G' and G'' appeared

successively, indicating that the internal structure of the emulsion collapsed, transitioning from a solid-like to a liquid-like state [13]. From the oscillatory shear strain corresponding to the intersection points of G' and G'' for samples prepared at different homogenization speeds, it can be seen that samples prepared at 8000 rpm and 10000 rpm could withstand higher shear without structural collapse. Samples prepared at low homogenization speeds had larger particle sizes and fewer emulsion particles per unit volume, resulting in weaker interactions between particles and thus lower shear tolerance. Samples prepared at high homogenization speeds exhibited higher solid-like behavior under low oscillatory shear due to partial aggregation of the internal phase. The dispersed phase particles in the system show a partially aggregated state (Figure 2a, Figure 2f). As the oscillatory shear strain increases, the aggregated solid oil structures are partially disrupted [14], leading to rheological behavior similar to that of low-homogenization samples (Figure 4b).

The temperature-dependent rheological behavior test results showed that emulsions prepared at high homogenization speeds had significantly lower tolerance to temperature during shear compared to those prepared at low homogenization speeds. This is likely because as the temperature approached the melting point of the oils, the exposed solid oils in the external phase softened or melted, directly causing the collapse of the system and a rapid transition to a liquid-like state, which led to the loss of system rigidity. In contrast, emulsions prepared at low homogenization speeds, with oils located within the dispersed phase, could still maintain some system rigidity through inter-particle interactions even after melting. This is crucial for the transportation stability of the product under extremely hot conditions.

4.3 Enhancement of Usage Feel and Efficacy by Process Parameters

From the sensory and moisturizing performance test results (Figure 5), it can be observed that process parameters have a significant impact on the usage feel and moisturizing properties of products with high-wax-content critical emulsification systems. In terms of sensory feel, emulsions prepared at medium and low homogenization speeds, with appropriate emulsifier coverage, are more conducive to the formation of liquid crystals. The water channels filled between the layers of the liquid crystalline structure allow for easy sliding between layers, thereby providing an excellent sensory feel when the cosmetic is applied [15]. In contrast, emulsions prepared at high homogenization speeds, due to partial aggregation between the internal phase emulsion particles, result in a coarser and heavier texture of the product. Therefore, they exhibit less smooth application, which is consistent with the description of the internal structure collapse of the emulsion in the rheological behavior test. Regarding moisturizing performance, samples prepared at medium and low homogenization speeds also benefit from the formation of liquid crystalline structures. The interlayer-bound water contained in the liquid crystalline structure, which evaporates slowly, plays an efficient moisturizing role [16].

5. Conclusion

This research integrated process optimization into product development to address the challenges in developing high-wax-content O/W critical systems. Consequently, it successfully

formulated products that meet the diverse needs of Chinese consumers while exhibiting excellent performance in withstanding extreme temperature variations.

References

[1] Hall-Manning TJ, Holland GH, Rennie G, et al. Skin irritation potential of mixed surfactant systems [J]. Food and Chemical Toxicology, 1998, 36(3): 233–238.

[2] Morris S, Xu L, Ananthapadmanabhan K, et al. Surfactant Penetration into Human Skin from Sodium Dodecyl Sulfate and Lauramidopropyl Betaine Mixtures [J]. Langmuir : the ACS journal of surfaces and colloids, 2021, 37(48): 14006-14014.

[3] Elik A, Yanik DK, Ozel B, et al. The effects of pectin and wax on the characteristics of oil-in-water (O/W) emulsions [J]. Journal of Food Science, 2021, 86: 3148-3158.

[4] Hua Z, Zhang C, He J, et al. Ultra-micro Liquid Crystal in Cosmetic Emulsion with Excellent Moisture Retention and Delivery Selectivity [J]. ACS Omega, 2024, 9(47): 47194-47202.

[5] Zhou P, Yang YF, Shen MM, et al. Experimental Analysis of the Interfacial Properties of Water-in-Heavy Oil Emulsions [J]. Mine Engineering, 2024, 13(1): 81-86.

[6] Ghosh S, Coupland JN. Factors affecting the freeze–thaw stability of emulsions [J]. Food Hydrocolloids, 2008, 22(1): 105-111.

[7] Yang Z, Jiang C, Xiang Q, et al. Probing the stability of emulsified asphalts: A dual analysis of zeta potential and particle size [J]. Fuel, 2025, 396(15): 135266.

[8] Sun N, Hu J, Shen L, et al. Effect of modified γ-Fe_2O_3 magnetic nanoparticles on the stability of heavy oil-in-water emulsions [J]. Journal of Dispersion Science & Technology, 2024, 45(9): 1829-1838.

[9] Liu C, Zheng Z, Cao C, et al. The partial coalescence behavior of oil-in-water emulsions: Comparison between refrigerated and room temperature storage[J]. Food chemistry, 2019, 300(1): 125219.

[10] Zhu YX. Study on emulsion stability and emulsification mechanism of eggplant pulp [D]. Nanjing Agricultural University, 2021.

[11] Rajagopal E S. The viscosity of polydisperse emulsions [J]. Rheologica Acta, 1961, 1(4): 581-584.

[12] Zhang Y, Chen W, Han YQ, et al. Recent advances in lamellar liquid crystal emulsification methods encapsulating natural active substances for functional cosmetics [J].Acta Pharmaceutica Sinica, 2024, 59(2): 350-358.

[13]Liu C , Zheng Z , Xi C ,et al. Exploration of the natural waxes-tuned crystallization behavior, droplet shape and rheology properties of O/W emulsions [J]. Journal of Colloid and Interface Science, 2020, 587(19): 417-428.

[14] Yang K. A study on the phenology of yield stress fluids in large amplitude oscillatory shear flow [D]. Shanghai Jiao Tong University, 2017.

[15] Chen YL. The Design and Research of Multifunctional Liquid Crystal Sunscreen Lotion [D]. Guangzhou: South China University of Technology, 2018.

[16] Liu HM, Ma XY, Zhao YH. Preparation of liquid crystal emulsion and its application in cosmetics [J]. China Surfactant Deterg Cosmet, 2022, 52: 762-769.